Supporting Information

Materials and Methods

Reagents and antibodies

N-Ethylmaleimide (NEM), tamoxifen, cycloheximide, 5-bromodeoxyuridine (BrdU), heparin, 4,6-diamidino-2-phenylindole (DAPI) and crystal violet were purchased from Sigma (Sigma-Aldrich). Protein A and G sepharose were obtained from GE Health Care. Isolectin B4-AF594 was purchased from Invitrogen. Complete-protease-inhibitor cocktail tablets were obtained from Roche. Recombinant human VEGFA and recombinant human FGF2 were obtained from PeproTech. The growth medium and FBS used for cell culture were obtained from Gibco (Life Technologies). The EGM-2 complete medium kits for primary endothelial cells were obtained from Lonza.

The following antibodies were used for immunoblotting (IB), immunoprecipitation (IP), and immunofluorescence (IF) staining were anti-FGFR1 (Cell Signaling Technology (CST), 9740, IB 1:2000, IP 1:200, and IF 1:100), anti-FLAG M2 (Sigma-Aldrich, A8592, IB 1:2000), anti-FLAG (CST, 8146, IF 1:200 and IP 1:200), anti-FLAG M2 magnetic beads (Sigma-Aldrich, M8823), anti-FRS2α (Abcam, ab183492, IB 1:2000 and IP 1:100), anti-HA (Roche, 11867423001, IP 0.2 μg per test), anti-HA (CST, 2999S, IB 1:1000), anti-Myc (Abmart, M20002, IB 1:3000), anti-actin (Sigma-Aldrich, A2228, IB 1:2000), anti-BrdU (Abcam, ab6326, IF 1:50), anti-PLCγ (Sangon Company, D155196, IB 1:1000), anti-SENP1 (Abcam, Ab10898, IB 1:2000 and IF 1:100), anti-SUMO1 (CST, 4390, IB 1:1000), anti-ERG (CST, 97249, IF 1:100), anti-VEGFR2 (CST, 2479, IB 1:2000), anti-VEGFR1 (CST, 2893, IB 1:1000), anti-p-FGFR1 (Tyr653/654) (CST, 3476, IB 1:1000), anti-p-FRS2α (Tyr436) (CST, 3861, IB 1:1000), anti-p-PLCγ (Tyr783) (CST, 2821, IB 1:1000), anti-p-ERK1/2 (Thr202/Tyr204) (CST, 9101, IB 1:2000), anti-p-VEGFR2 (Tyr1054/1059) (CST, 3817, IB 1:2000 and IF 1:50). Horseradish peroxidase-linked anti-rabbit IgG secondary antibody (Jackson ImmunoResearch, #711-035-152, 1:10,000), anti-mouse IgG secondary antibody (Jackson ImmunoResearch, #715-035-151, 1:10,000) and anti-goat IgG secondary antibody (Jackson ImmunoResearch, #705-035-147, 1:10,000) were used for IB. Alexa Fluor 594-conjugated donkey anti-rabbit IgG (Jackson ImmunoResearch, #711-586-152, 1:200), Alexa Fluor 594-conjugated donkey anti-rat IgG (Jackson ImmunoResearch, #712-586-150, 1:200) and Alexa Fluor 488-conjugated donkey anti-goat IgG (Jackson ImmunoResearch, #705-545-147, 1:200) were used for IF staining, and DAPI was used to stain nuclei.

Cell lines and culture conditions

All the cell lines were cultured in a humidified 37°C incubator with 5% CO2. HEK293T cells and COS-7 cells were cultured in Dulbecco's modified Eagle's medium (DMEM, Gibco 11965084) with 10% fetal bovine serum (FBS, Gibco) and 100 U/ml penicillin/streptomycin (Gibco 15140122). Human microvascular endothelial cells (HMVECs) and human umbilical vein endothelial cells (HUVECs) were purchased from Lonza and maintained in EBM-2 (Lonza) supplemented with 2% FBS, 2 mM L-glutamine, 100 U/ml penicillin/streptomycin and EGM-2 bullet kits. Primary mouse lung endothelial cells (MLECs) from 8-week-old mice were isolated and cultured in complete EGM-2 growth medium. The cells were maintained at 30%–90% confluence and were subcultured using 0.05% trypsin-EDTA (Gibco 25300120) for dissociation. Cellular stress conditions were induced by treatment with VEGFA at 10 ng/ml or FGF2 at 100 ng/ml in the presence of 20 U/ml heparin for the indicated time points after serum free starvation for 4 h. Hypoxia was induced by transferring cells into a hypoxic incubator containing 1% O2, 5% CO2

and 94% N2 and incubating them for 12 h. All experimental primary endothelial cells were used through passage 7.

Plasmids and transfection

The expression plasmid for Flag-tagged FGFR1-WT was obtained from YouBio (G114229). All FGFR1 mutations were generated by site-directed mutagenesis in which Lys 517 and Lys 714 were changed to Arg residues and were verified by DNA sequencing. A SUMO-1 fusion plasmid was constructed similarly to that generated for expressing SUMOylated proteins(31, 35). Briefly, the PCR-amplified SUMO1 fragment (without a double glycine-encoding sequence at the C-terminal) was subcloned into a pXF6F vector plasmid using restriction sites BglII and NotI. Then, PCR-amplified human FGFR1 cDNA was subcloned into the restriction sites XhoI and XbaI in the C-terminal domain of the SUMO1 fragment. Expression plasmids for HA-SUMO1, Myc-SENP1-WT, Myc-SENP1-CA mutant (SENP1-Mut), HA-SENP1-WT, HA-SENP2-WT, HA-SENP5-WT, and VEGFR2 were thus constructed in our laboratory. HA-Frs2α-full-length was obtained from YouBio (G111928), and HA-Frs2α-PTB and HA-Frs2α-ΔPTB were constructed based on this vector. The PTB domain consists of amino acids 18-110, while HA-Frs2α-ΔPTB consists of amino acids 1-17 and 111-508. HA-PTPRG was obtained from YouBio (G156730).

293T or COS-7 cells were seeded into 6-well plates the day before transfection and cultured until they reached 50-70% confluence, and then, they were transfected. Plasmids transfection was performed using Lipofectamine 2000 (Life Technologies) according to the manufacturer's protocol. Cells were treated and harvested for protein assays or immunofluorescence staining 24 to 48 h after transfection.

siRNA transfection

Endothelial cells were seeded into 6-well plates or 100-mm dishes 16 h prior to transfection and allowed to grow to 50-70% confluence and then were transfected. siRNAs or scrambled siRNA were transfected using Lipofectamine RNA iMAX according to the manufacturer's instructions (Life Technologies) in reduced serum medium Opti-MEM (Life Technologies). Cells were transfected with siRNAs for 72 h before cellular stress treatment. The sequences of the siRNAs were SENP1, 5'-GUGAACCACAACUCCGUAUUCTT-3'; FGFR1, 5'-CAAAUGCCCUUCCAGUGGGTT-3'; PTPRG, 5'-GCUAAUACCACUCGAAUAUTT-3'; and negative control, 5'-UUCUCCGAACGUGUCACGUTT-3'.

Adenovirus infection

Several adenoviruses were generated (Ad-SENP1-WT, Ad-SENP1-CA, Ad-Flag-FGFR1-WT, Ad-Flag-FGFR1-2KR, and Ad-Flag-FGFR1-SUMO1) to overexpress SENP1, the SENP1 CA mutant, FGFR1-WT, the FGFR1-2KR mutant, and Flag-FGFR1-SUMO1 in endothelial cells. Adenoviral vectors containing SENP1-WT, SENP1-CA mutant, Flag-FGFR1-WT, Flag- FGFR1-2KR mutant, and Flag-FGFR1-SUMO1 were generated by inserting the corresponding cDNA into a multicloning site in the adenovirus backbone of plasmid pHBAD. The constructs were cotransfected with shuttle vectors into 293 cells for adenovirus packaging and amplification and then purified (Hanbio Biotech Company, Shanghai, China). endothelial cells were first transfected with SENP1 siRNA or FGFR1 siRNA to knockdown the endogenous expression of SENP1 or FGFR1 before they were transduced with Ad-SENP1, Ad-SENP1-CA, Ad-Flag-FGFR1-WT, or Ad-Flag-FGFR1-2KR. Twenty-four hours after siRNA transfection, the cells were infected with various adenoviruses at an MOI of 30-50 in Opti-MEM (Gibco) and incubated for 4 h. Then, the

cells were maintained in EGM-2 complete culture medium for an additional 48 h before assays were performed.

Cell lysates and cell fractionation

Cells were washed with ice-cold PBS and lysed in Triton lysis buffer (50 mM Tris-HCL, pH 7.5; 150 mM NaCl; 1 mM EDTA; 1 mM EGTA; and 0.1% (v/v) Triton X-100); and 1x protease inhibitor cocktail) for 20 min on ice and centrifuged (14,000 rpm for 10 min at 4°C). Then, 5x/2x SDS sample buffer (250 mM Tris, 5%/2% SDS, 50% glycerol and 500 mM/200 mM DTT) was added to the lysate to a final concentration of 1x. After heating for 5 min at 100°C, samples were placed in ice and cooled for use. Cell fractionation was conducted using a subcellular protein fractionation kit (Pierce) according to the manufacturer's instructions.

Immunoblotting

Cellular proteins or IP samples were analyzed directly by electrophoresis. Lysates or immunoprecipitates were run on SDS-PAGE gels (8%/10%/12%) and transferred to polyvinylidene fluoride membranes (Bio-Rad Laboratories). The membranes were blocked with 5% skim milk and TBST for 1 h at room temperature, briefly rinsed with TBST and then incubated overnight with primary antibody at 4°C. After washing, the membranes were incubated with secondary antibody for 1 h at room temperature and then washed again three times. Finally, chemiluminescence was detected using ECL reagents.

Protein stability assay

The stability of FGFR1-WT and FGFR1-2KR was determined by cycloheximide (CHX) treatment. In brief, plasmids encoding Flag-tagged FGFR1 or the FGFR1-2KR mutant were transfected into 293T cells, incubated 24 h and treated with 10 μM CHX treatment at the indicated time points. The cell lysate was harvested at the indicated time point and subjected to immunoblotting analysis. Flag-FGFR1-WT and Flag-FGFR1-2KR were measured with actin used as an internal control.

Quantitative real-time PCR

Total RNA was harvested according to the instructions of a kit (Omega). After quantification, 500 ng of RNA was reverse transcribed to cDNA according to the protocol of a reverse transcription kit (TaKaRa) followed by quantitative real-time PCR on an iCycler real-time PCR detection system (Bio-Rad). GAPDH was used as an internal control. The sequences of the primers (5'-3') were

PTPRG, forward TTCGTGTGCCTCATCCTTCT and reverse TCGAGGTGAACTGCTGTCTT and

GAPDH, forward CATTGCCCTCAACGACCACTTTGT and reverse:
TCTCTCTCTTCCTCTTGTGCTCTTGC.

Immunofluorescence staining

The subcellular localization of FGFR1-WT and FGFR1-2KR was determined by immunofluorescence staining. COS-7 cells transfected with 1 μg of Flag-FGFR1-WT or 1 μg of Flag-FGFR1-2KR were washed with PBS, fixed in 4% PFA for 10 min at room temperature, blocked with blocking buffer (PBS with 5% (v/v) goat FBS and 1% (w/v) BSA) for 1 h at room temperature, and incubated overnight with primary antibody at 4°C. Secondary antibody conjugated with Alexa Fluor 488 was incubated for 1 h at room temperature, and nuclei were stained with DAPI. All sections were mounted and imaged using a confocal microscope (Zeiss, AxioVert 200 M).

MLEC isolation

Lungs from FGFR1-WT^{ecKI} and FGFR1-2KR^{ecKI} mice were harvested, minced, and digested with prewarmed 0.1% collagenase in PBS containing Ca2+ and Mg2+ for 1 h at 37°C. The digest was homogenized by passing it 15 times through a 16-gauge needle and was then filtered through a 70-μm tissue sieve into a 50-ml tube. After centrifugation, the digest was resuspended in growth medium (EGM-2 full medium) and then seeded on 0.1% gelatin-coated tissue culture dishes. After 3 to 4 days of culture in growth medium, endothelial cells were isolated by magnetic beads (IgG Dynal beads from Dynal Corp., Great Neck, NY) preconjugated with anti-ICAM-2 antibody and separated by a magnetic separator. A second sorting process was performed after 4-5 days of culture. The cells immunoselected twice were used for subsequent experiments.

Supplemental Figures

A

Position	Peptide	Score
160	SP EKME K	3.926
517	KM LKSD A	3.25
714	KL LKEG H	2.662

(By SUMOsp 2.0)

Position	Peptide	Score
517	VAVKM LKSD ATEKD	0.91
198	KNGKE FKPD HRIGG	0.85
177	AKTVK FKCP SSGTP	0.74
714	ELFKL LKEG HRMDK	0.73

(By SUMOplot™ Analysis Program)

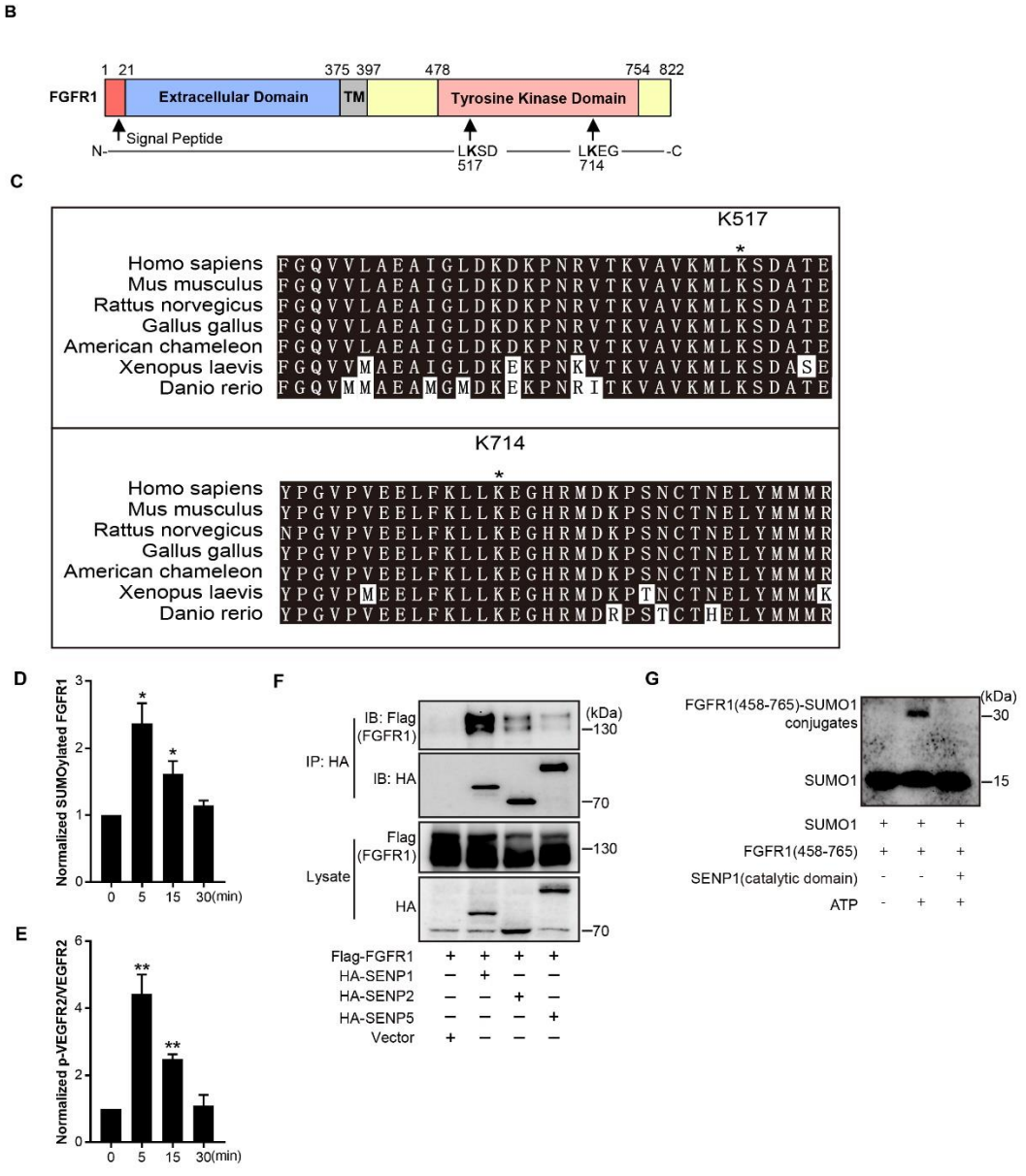

Figure. S1. The prediction and conservation of SUMOylation sites in the FGFR1 protein and the interaction between FGFR1 and SENP proteins. A The putative SUMOylation sites in FGFR1 were determined by SUMOsp2.0 software and SUMOplot™ Analysis Program online

tools. Two lysine residues (lysine 517 and lysine 714) were consistent in the results. **B** Mapped domains of the FGFR1 protein and the relevant position of lysine 517 and lysine 714 residues. **C** Alignment of orthologous FGFR1 amino acid sequences in *Homo sapiens*, *Mus musculus*, *Rattus norvegicus*, *Gallus gallus*, American chameleon, *Xenopus laevis*, and *Danio rerio* demonstrates evolutionary conservation of SUMOylation sites in FGFR1. **D-E** Quantification of FGFR1 SUMOylation and VEGFR2 phosphorylation for Fig. 1F. The relative SUMOylated FGFR1 and p-VEGFR2/VEGFR2 are presented as mean ± SEM (n=3). *, p≤0.05; **, p≤0.01. **F** Representative blot showing the association between FGFR1 and SENP proteins. Flag-FGFR1 plasmids were co-transfected with HA-vector, HA-SENP1, HA-SENP2, or SENP5. HA (SENP) was immunoprecipitated followed by immunoblotting using anti-Flag (FGFR1) antibody. **G** FGFR1 SUMOylation was de-SUMOlated by recombinant SENP1 in an *in vitro* SUMOylation assay. The assay was performed using a SUMOylation assay kit as described in the “Materials and Methods” section. The reaction mixture was subjected to immunoblotting with anti-SUMO1 antibody as indicated.

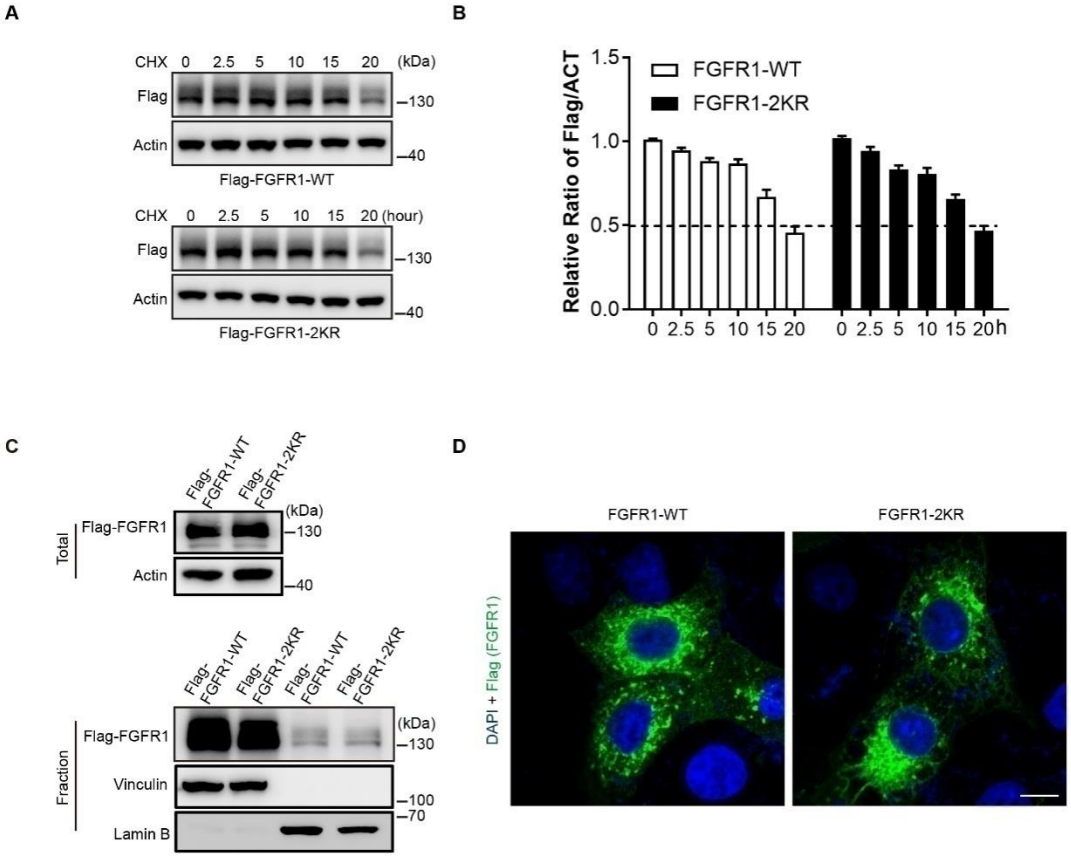

Figure. S2. The protein stability and intracellular localization of FGFR1-WT and the FGFR1-2KR mutant. A-B Half-life test of FGFR1-WT and FGFR1-2KR. 293T cells were transfected with Flag-FGFR1-WT or Flag-FGFR1-2KR mutant plasmids followed by cycloheximide (CHX, 10 μg/ml) at the indicated time points. The expression of Flag-FGFR1-WT or Flag-FGFR1-2KR was determined by anti-Flag antibody. The blots are shown in (**A**), and the quantification of the relative protein levels are presented as mean ± SEM (n=3) in (**B**). **C-D** Distribution of FGFR1-WT and FGFR1-2KR. The expression of FGFR1-WT and FGFR1-2KR in the cytoplasm and nucleus was detected by anti-Flag antibody after cell fractionation (**C**) or immunofluorescence staining using an anti-Flag antibody (**D**). The nuclei were stained with DAPI. The bar represents 25 μm.

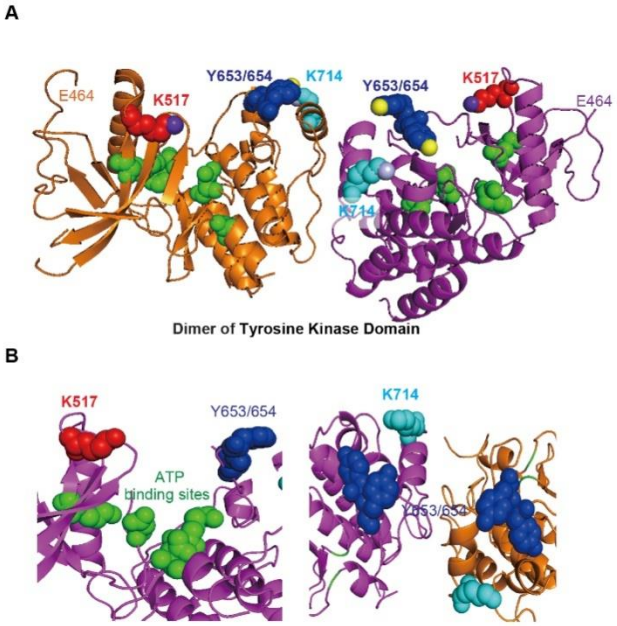

Figure. S3. Lysine 517/714 in the FGFR1 tyrosine kinase domain. The crystal structure of the dimerized human FGFR1 tyrosine kinase domain (1AGW in the PDB database) was displayed by PyMOL software 1.5.0.3. **A** Two putative SUMO1 binding site residues, K517 (red) and K714 (light blue) reside in the core autophosphorylation region of the FGFR1 tyrosine kinase domain and are present on the surface of each subunit. **B** The details of the structure around K517 and K714 demonstrate that the K517 residue is located close to an ATP-binding pocket, which contains more than 5 ATP-binding sites, providing the phosphate group for the FGFR1 protein, and the K714 residue is located near the dimer interface of juxtaposed tyrosine kinase domains and close to the core tyrosine residues Tyr653/654, which are essential for the catalytic activity and signal transduction of FGFR1.

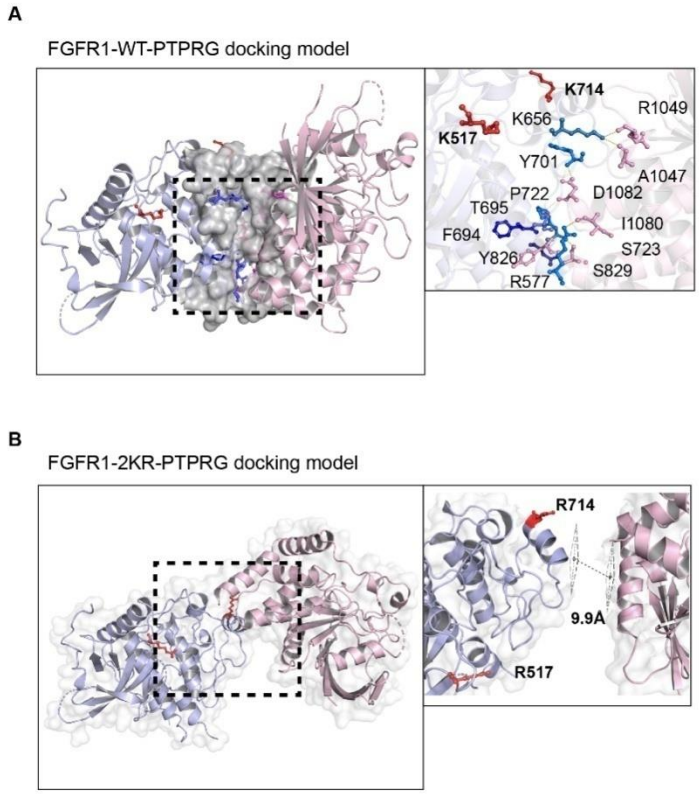

Figure. S4. The conformational changes triggered by deSUMOylation of FGFR1 restrain its interacting and docking capabilities with PTPRG. The molecular docking of FGFR1-WT and FGFR1-2KR tyrosine kinase domains with the PTPRG tyrosine-protein phosphatase domain was assessed by GrammX and Z-DOCK algorithms. The distances (Å) and docking interface between FGFR1-WT/FGFR1-2KR and PTPRG were measured and performed by PyMOL 2.3.0 open-source software. The 3D structures of FGFR1-WT and FGFR1-2KR (general view and at specific residues) are labeled in light blue in (**A-B**); the PTPRG (general view and at specific residues) are labeled in light pink in (**A-B**); the interacting residues of the docking interface are indicated by the black dashed boxes in the left panels of (**A-B**), which are enlarged in the right panels of (**A-B**); the SUMOylated/deSUMOylated residues (K517/R517, K714/R714) are labeled in red, the residues of FGFR1 in the docking interface are labeled in blue, the residues of PTPRG in the docking interface are labeled in pink; the molecular binding force of the hydrogen bonds is indicated as yellow dashed lines in the right panels in (**A-B**). Compared to FGFR1-WT, FGFR1-2KR interacts with much lower binding affinity for PTPRG. Hydrogen bonds are the molecular binding forces of FGFR1-WT with PTPRG, with interacting residue distances less than 3 Å, whereas the distance between FGFR1-2KR and PTPRG at the docking interface is 9.9 Å.

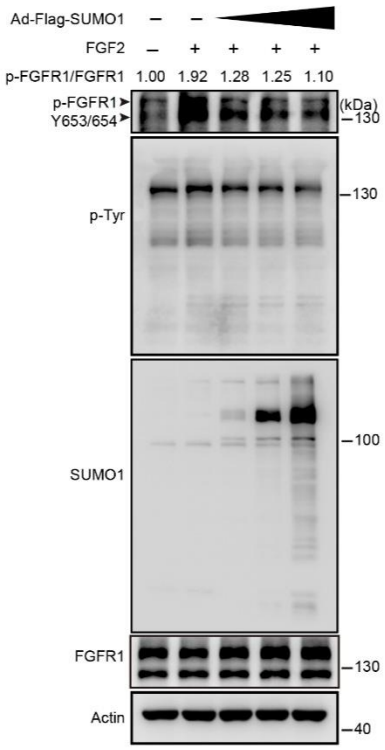

204

205 **Figure. S5. Phosphorylation of FGFR1 (Y653/654) is suppressed in endothelial cells**
206 **following an increase in SUMOylation.** Representative blot showing p-FGFR1 (Y653/654) and
207 p-Tyr. Ad-GFP or Ad-Flag-SUMO1 was transduced into endothelial cells followed by FGF2
208 stimulation for 5 min after serum free starvation. Arrowhead indicates band of interest.

209

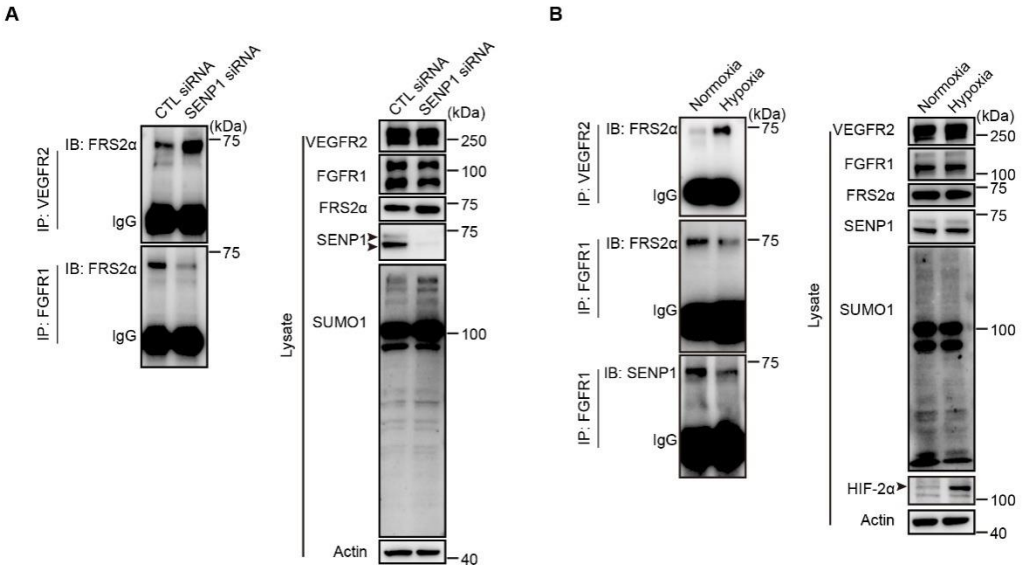

Figure. S6. SENP1 knockdown or hypoxia enhances VEGFR2-FRS2α association but inhibits FGFR1-FRS2α association in endothelial cells. Representative blots of FRS2α that co-immunoprecipitates with FGFR1 and VEGFR2 upon control siRNA/SENP1 siRNA treatment (A) or normoxia/hypoxia treatment (B) in HMVECs with 16h starvation. Arrowhead indicates band of interest.

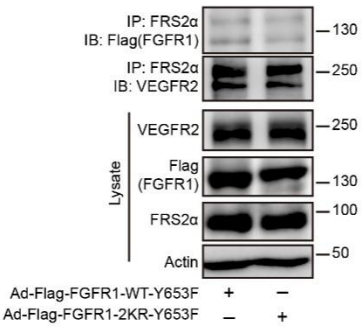

Figure. S7. Y653/654 inactivation in FGFR1 eliminates the differences in the binding of FGFR1-WT or FGFR1-2KR with FRS2α and in corresponding VEGFR2-FRS2α association. FRS2α was immunoprecipitated followed by immunoblotting for FGFR1(Flag) and VEGFR2 in HMVECs transduced with adenoviral-delivered FGFR1-WT-Y653F (Ad-Flag-FGFR1-WT-Y653F) or FGFR1-2KR-Y653F (Ad-Flag-FGFR1-2KR-Y653F) mutants. Representative blots of binding of FRS2α to FGFR1 or VEGFR2 are shown.

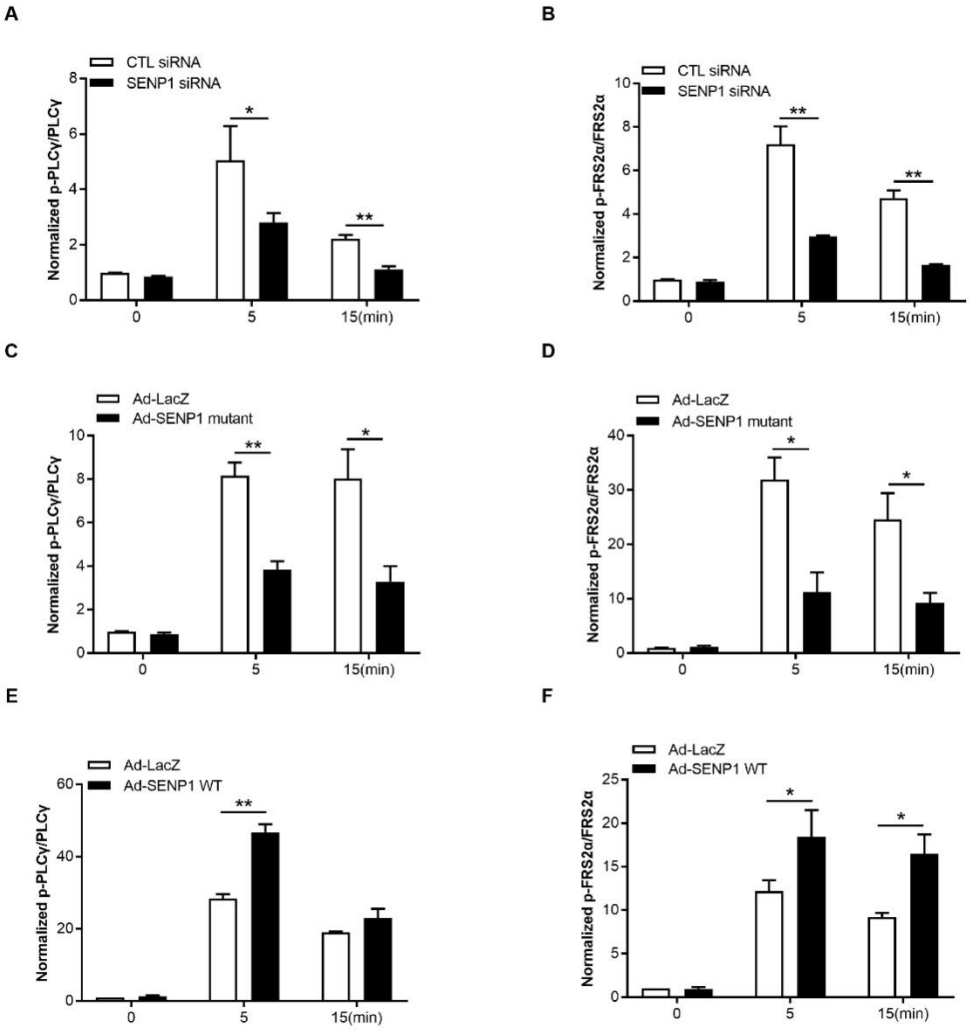

Figure. S8. Quantification of FGFR1 downstream signaling activation in endothelial cells with SENP1 knockdown or WT/mutant overexpression. FGF2 induced PLCγ phosphorylation and FRS2α phosphorylation in control/SENP1 siRNA treated HMVECs (A-B), Ad-LacZ/Ad-SENP1 mut treated HMVECs (C-D), and Ad-LacZ/Ad-SENP1 WT treated HMVECs (E-F) at indicated time points were quantified, respectively. Normalized value is presented as mean ± SEM from three independent experiments. *, p≤0.05; **, p≤0.01.

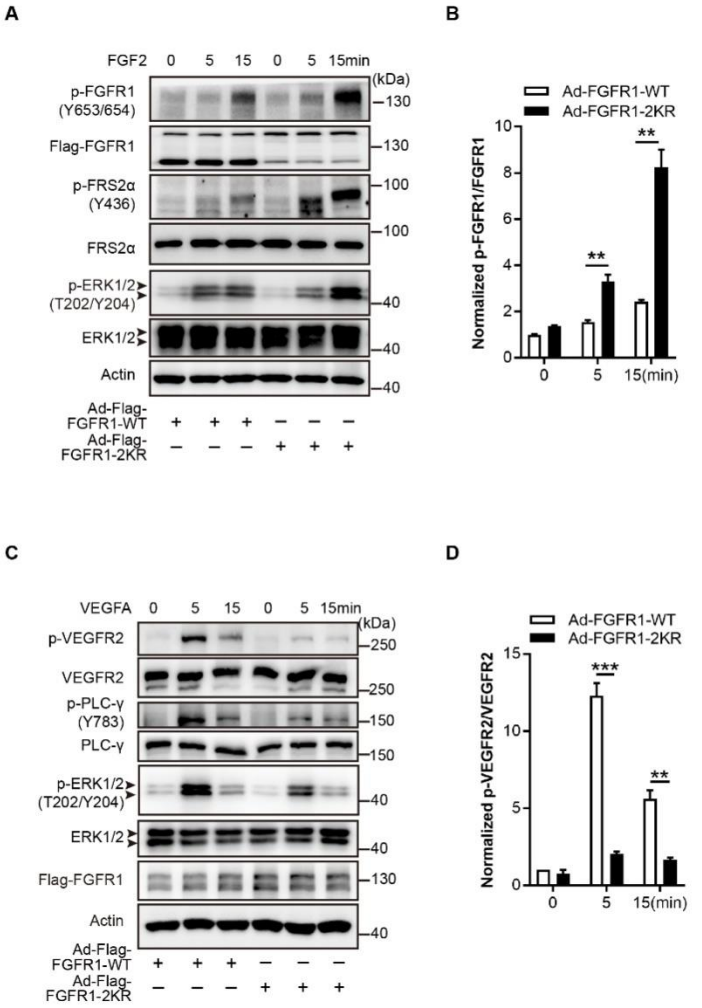

Figure. S9. FGF2-FGFR1 signaling and VEGFA-VEGFR2 signaling in HUVECs expressing FGFR1-WT or the FGFR1-2KR mutant. A-B FGF2-FGFR1 signaling in HUVECs infected with Ad-FGFR1-WT or the Ad-FGFR1-2KR mutant after FGF2 stimulation at the indicated time points. Representative blots are shown in **A** with quantification of p-FGFR1/FGFR1 in **B.** Arrowhead indicates band of interest. **C-D** VEGFA-VEGFR2 signaling in HUVECs infected with Ad-FGFR1-WT or the Ad-FGFR1-2KR after VEGFA stimulation at the indicated time points. Representative blots are shown in **C** with quantification of p-VEGFR2/VEGFR2 ratio in **D.** Arrowhead indicates band of interest. The normalized amount in **B** and **D** are presented as mean ± SEM (n=3). **, p≤0.01; ***, p≤0.001.

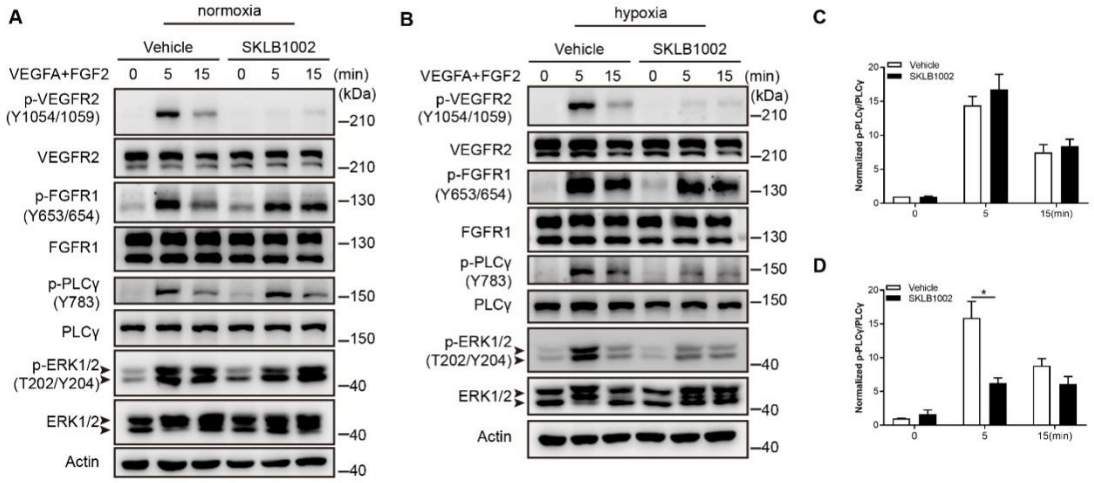

Figure. S10. The activation of FGF2-FGFR1 signaling and VEGFA-VEGFR2 signaling in endothelial cells with SKLB1002 treatment under normoxia and hypoxia. (A, C) FGF2-FGFR1 signaling and VEGFA-VEGFR2 signaling in HMVECs treated with vehicle or SKLB1002 (VEGFR2 signaling inhibitor) under normoxia. Representative blots are shown in **A** with quantification of PLCγ phosphorylation in **C**. **(B, D)** FGF2-FGFR1 signaling and VEGFA-VEGFR2 signaling in HMVECs treated with vehicle or SKLB1002 under hypoxia. Representative blots are shown in **B** with quantification of PLCγ phosphorylation in **D**. The quantification data are presented as the mean ± SEM (n=3), *, p≤0.05. Arrowhead indicates band of interest.

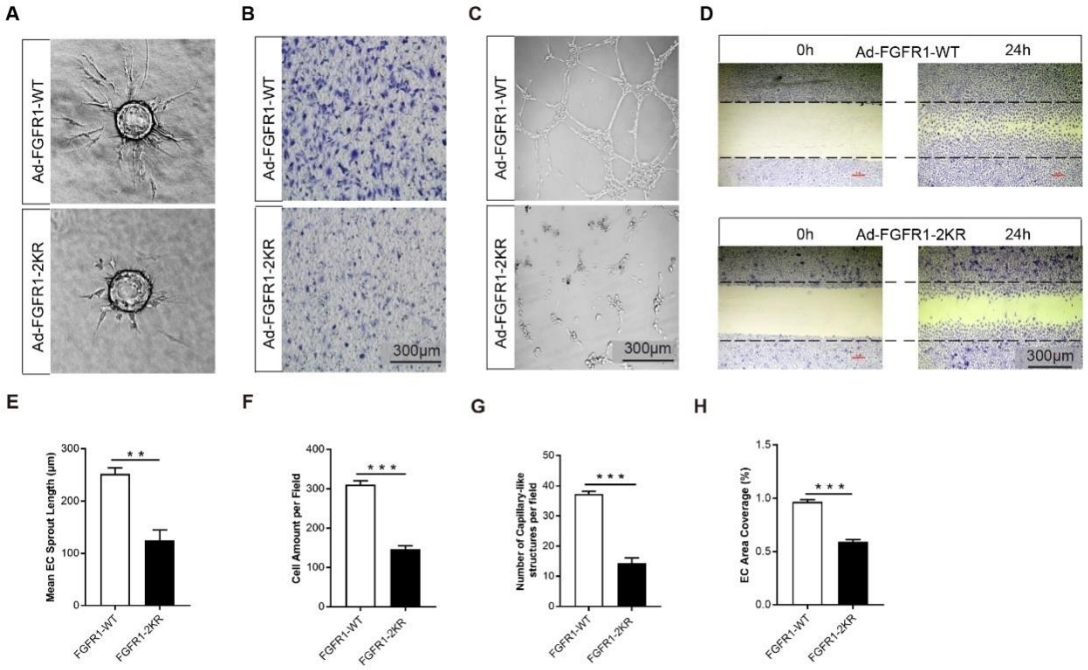

Figure. S11. The angiogenic capabilities of endothelial cells bearing the FGFR1-2KR mutant are blocked. HUVECs infected with Ad-FGFR1-WT or the Ad-FGFR1-2KR mutant were evaluated for proangiogenic capabilities. Representative images of sprouting, transmigration, capillary-like structure formation, and wound healing are shown in **A-D**. The quantification of EC sprout length, number of migrated cells, number of capillary-like structures, and EC area coverage are shown in **E-H**. All experiments were performed in triplicate, and significance was determined by unpaired t-test. The data are presented as the mean ± SEM from at least three independent experiments, where **, $p \leq 0.01$ and ***, $p \leq 0.001$. The bar represents 300 μm.

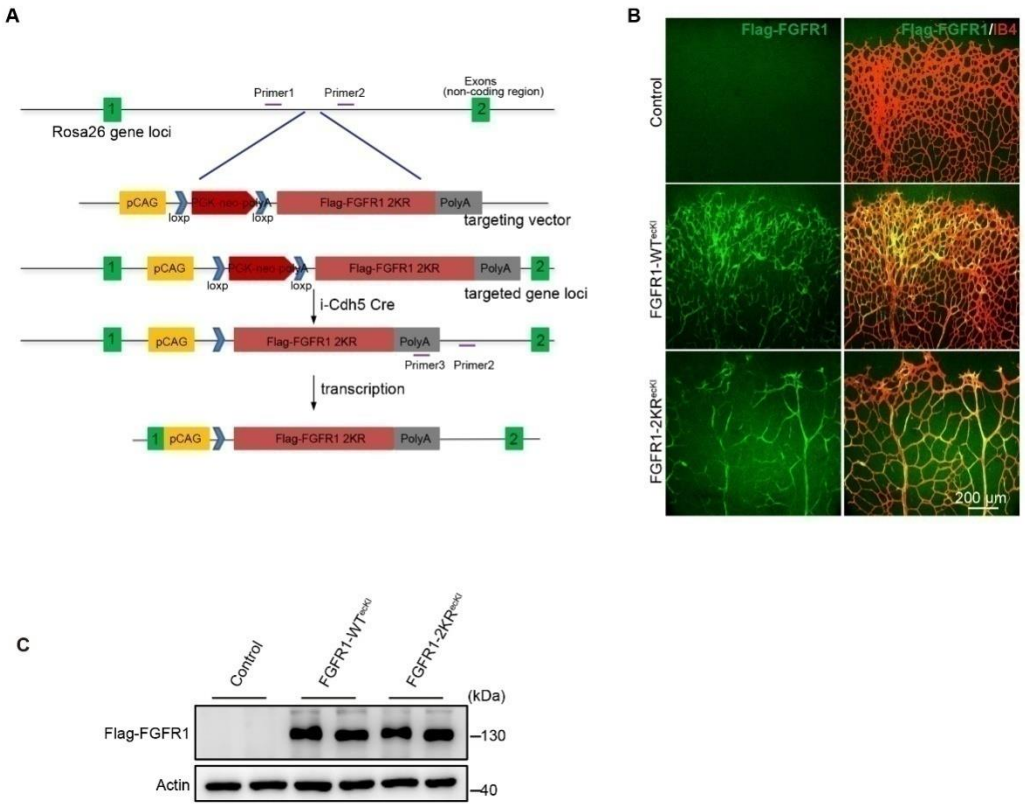

Figure. S12. Construction of inducible endothelial FGFR1-WT/FGFR1-2KR mutant knock-in mice. A construction strategy. The cDNA-encoding Flag-tagged FGFR1 wild-type (FGFR1-WT) protein coding sequence was inserted downstream of a loxP-flanking transcriptional stopper cassette (PGK-neo-polyA). This fragment was targeted to a constitutively transcribing ROSA26 locus to generate FGFR1-WT ROSA26 knock-in mice, which were bred with Cdh5-CreERT2 (iCdh5 Cre) mice to obtain inducible endothelial-cell-specific FGFR1-WT (FGFR1-WT^{ecKI}) expression upon tamoxifen injection. The same strategy was employed for the construction of tamoxifen-inducible endothelial cell-specific expression of the FGFR1 2KR mutant (FGFR1-2KR^{ecKI}). **B** Tamoxifen induced the expression of FGFR1-WT (Flag) (green) and FGFR1-2KR (Flag) (green) in vasculature stained by IB4-594 in whole-mount P7 retinas from the control (n=3) or FGFR1-WT^{ecKI} (n=4) or FGFR1-2KR^{ecKI} mice (n=3). The bar represents 200 μm. **C** Protein levels of FGFR1-WT and FGFR1-2KR. After intraperitoneal injection of tamoxifen, primary endothelial cells were isolated from the lung tissue of transgenic mice, and the protein levels of FGFR1-WT (Flag) and FGFR1-2KR (Flag) were detected by anti-Flag antibody.

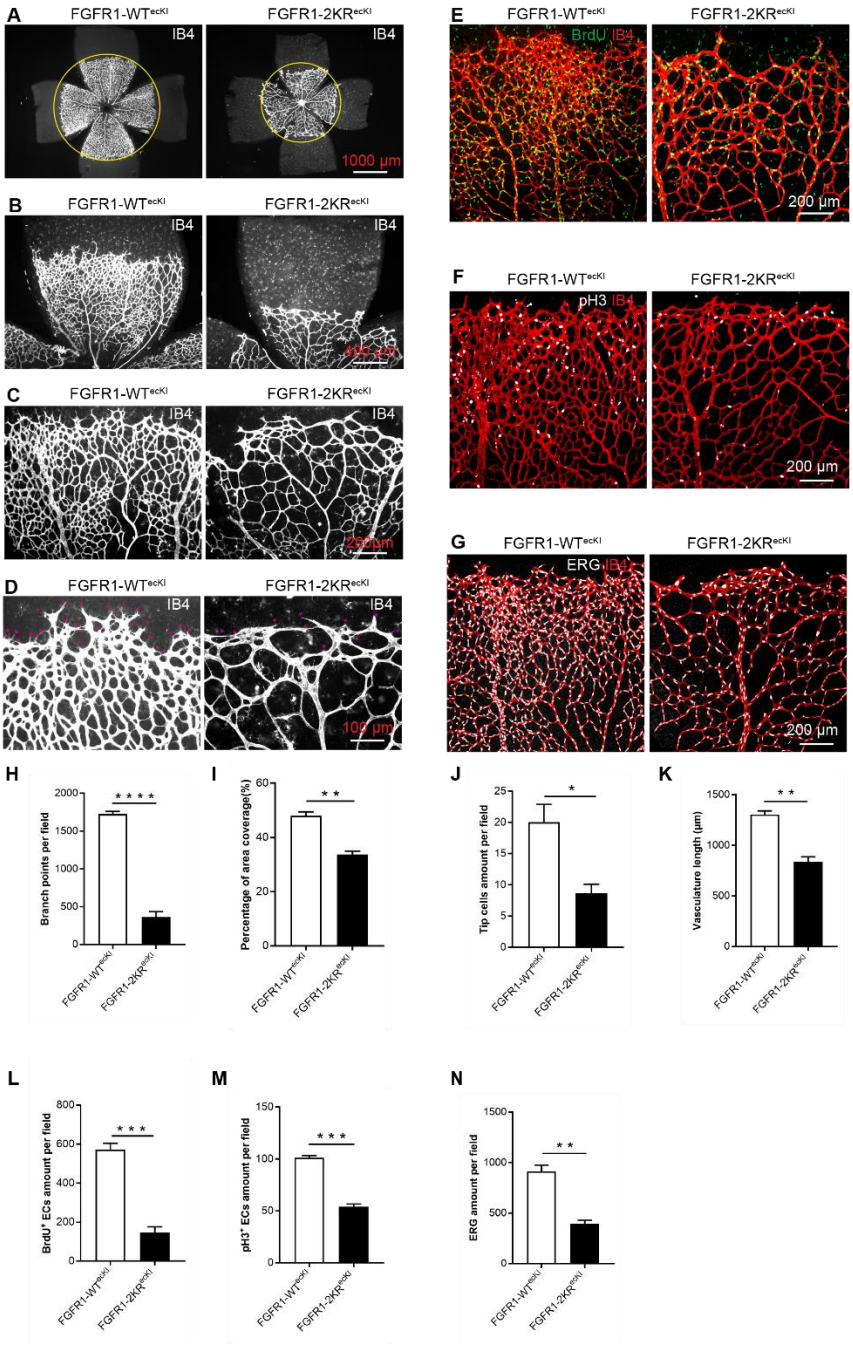

285
286 **Figure. S13. Neonatal retina angiogenesis and proliferation analysis in P5 FGFR1-WT^{ecKI}-**
287 **and FGFR1-2KR^{ecKI}-expressing pups. A-D** Whole-mount P5 retinas from FGFR1-WT^{ecKI}- or
288 FGFR1-2KR^{ecKI}- expressing mice. Representative images of P5 vascular outgrowth in FGFR1-
289 WT^{ecKI} control (n=10) and FGFR1-2KR^{ecKI} retinas (n=12) stained with IB4 are shown. Red
290 asterisks in **D** indicate tip cells. **E-G** Proliferation test of endothelial cells in the P5 FGFR1-WT^{ecKI}
291 (n≥4 for all assays) and P5 FGFR1-2KR^{ecKI} (n≥4 for all assays) retinal vasculature. BrdU (**E**) and
292 phospho-histone H3 (**F**) staining intensities were analyzed to determine the proliferation capability
293 of endothelial cells in the FGFR1-WT^{ecKI}- and FGFR1-2KR^{ecKI}–expressing pups. ERG (**G**) staining

intensity was measured to indicate the number of endothelial cells in the retinal vasculature. **H-N** Quantification of all the experiments above. All experiments were performed in triplicate, and significance was determined by unpaired t-test. The data are presented as the mean ± SEM, where *, $p \leq 0.05$, **, $p \leq 0.01$, ***, $p \leq 0.001$, ****, $p \leq 0.0001$.

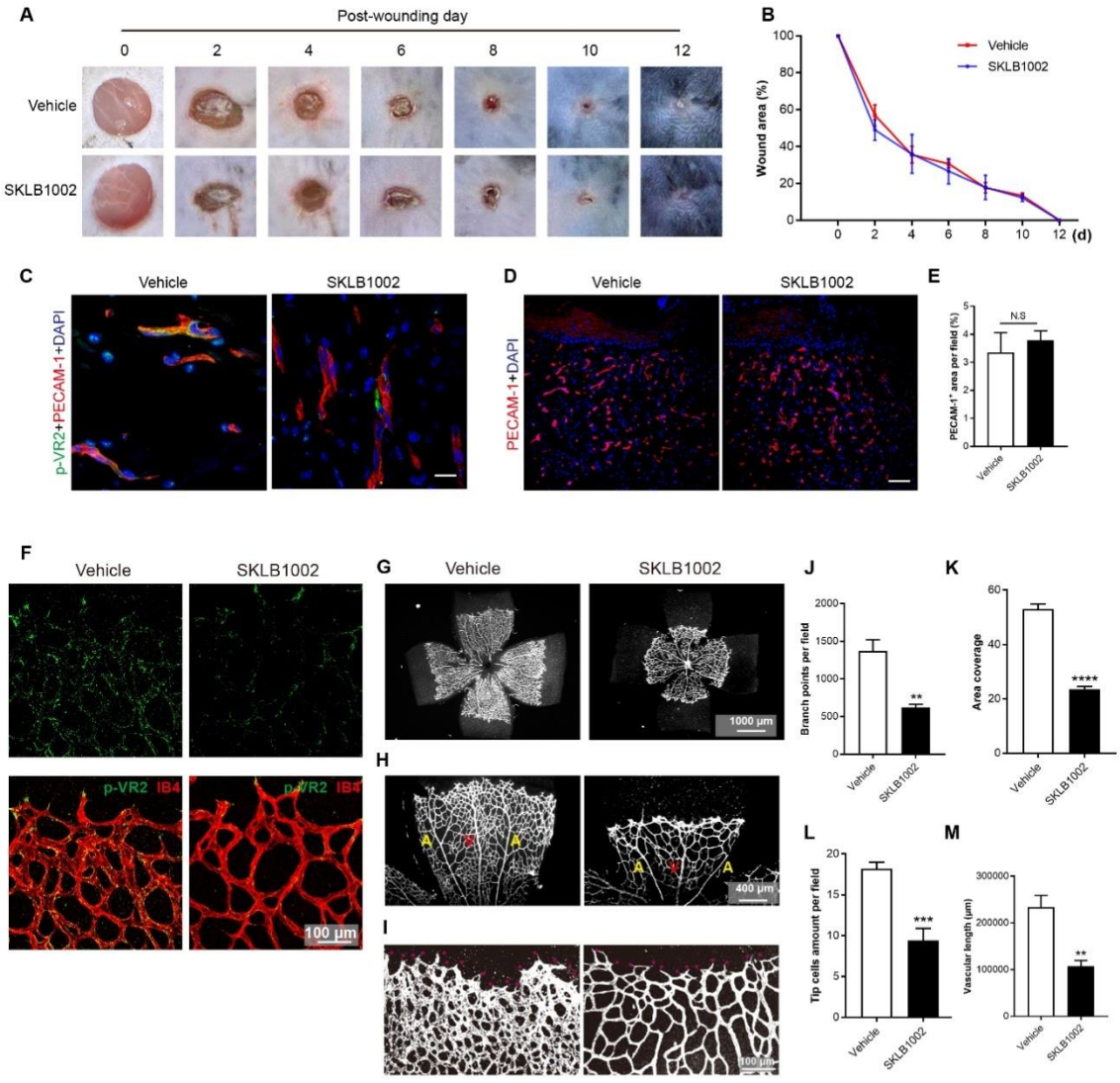

Figure. S14. The VEGFR2 signaling inhibitor does not affect wound angiogenesis but suppresses neonatal retinal angiogenesis in mice, suggesting the critical role of FGFR1

signaling in pathological angiogenesis under normoxia and VEGFR2 signaling in hypoxic angiogenesis. (A-B) Skin wound healing of mice treated with vehicle (n=5) or SKLB1002 (VEGFR2 signaling inhibitor) (n=5). Representative images of skin wound from day 0 to day 12 after wound injury are shown in **A** with quantification of wound area in **B**. Data are shown as mean ± SEM. Significance was determined by two-way ANOVA followed by Bonferroni's multiple comparisons test. **(C)** Representative images of immunofluorescence staining for p-VEGFR2 (green) and endothelial marker PECAM-1 (red) in skin section from mice treated with vehicle or SKLB1002. DAPI was used to indicate nuclear. Bar represents 50 μm. **(D)** Representative PECAM-1 labeled vessels (red) in wound edge of vehicle or SKLB1002-treated mice 6 days after excision wound injury. Nuclei is stained by DAPI (blue). Bar represents 200 μm. **(E)** Quantitative immunofluorescence of PECAM-1 positive area (vessel area) per field in **D**. Comparison was performed by t-test. N.S = non significance. **(F)** Representative images showing p-VEGFR2 (green) in the vehicle and SKLB1002 treated retinal vasculature with IB4 staining in red. **(G-I)** Representative images showing P5 vascular outgrowth in vehicle control (n=5) or SKLB1002 treated mouse retinas (n=5) stained with IB4. "A" in **H** indicates artery, while "V" indicates vein. Red asterisks in **I** indicate tip cells. **(J-M)** The quantification data of the branch points, area coverage, tip cell amounts, and vasculature length are presented as the mean ± SEM (n=5). Significance was determined by an unpaired t-test. **, $p \leq 0.01$; ***, $p \leq 0.001$; ****, $p \leq 0.0001$.